



GONÇALO GARCÊS SOBREIRA RODRIGUES BAPTISTA
BSc in Physics Engineering

X-RAY RESONANT RAMAN SCATTERING

SPECTRA SIMULATION FROM FIRST PRINCIPLES
FOR COPPER BELLOW IONIZATION THRESHOLD
USING HIGH-PERFORMANCE COMPUTING

MASTER IN PHYSICS ENGINEERING

NOVA University Lisbon

Draft: February 19, 2023

X-RAY RESONANT RAMAN SCATTERING

SPECTRA SIMULATION FROM FIRST PRINCIPLES
FOR COPPER BELOW IONIZATION THRESHOLD
USING HIGH-PERFORMANCE COMPUTING

GONÇALO GARCÊS SOBREIRA RODRIGUES BAPTISTA

BSc in Physics Engineering

Advisers: Jorge Felizardo Machado

Auxiliary Professor, NOVA University Lisbon

Mauro António Guerra

Auxiliary Professor, NOVA University Lisbon

Abstract

The work performed on this thesis comes as part of the effort to further understand the highly convoluted structure present on Copper's x-ray emission spectra, where, as with many other transition metals, a skewness can be observed on the $K_{\alpha_{1,2}}$, K_{β} and L transition lines. These line originate due to the radiative relaxation of the atom's electronic structure post-ionization of inner shell electrons. However, it is possible that the observed skewness is due to copper's satellite states' transitions.

Throughout this thesis, a study will be performed for the satellite states formed by the excitation of the inner-shell electron, where the ionization process did not occur.

Multiple atomic structure calculations will be performed using the *ab initio* state of the art [Multiconfiguration Dirac-Fock General Matrix of Elements \(MCDFGME\)](#) code for different excited states configurations (from an electron in the 4s orbital up to $n=??$).

The obtained results will then be used in the analysis of experimental data obtained from a High-Precision [Double Crystal Spectrometer \(DCS\)](#), located in Paris, in a synchrotron line.

Due to the complexity of the calculations, the process can become quite hefty in terms of computational power and time. Therefore, further similar and more complex studies will be performed by implementing and running a script in the *Oblivion* supercomputer located at the University of Évora.

Keywords: Excited State, Diagram Lines, [MCDFGME](#), [DCS](#), High Performance Computing

Resumo

asdasdasdas asdasdasdas
asdasdasdasa
asdasdasdas

Palavras-chave: Primeira palavra-chave, Outra palavra-chave, Mais uma palavra-chave,
A última palavra-chave

Contents

List of Figures	v
List of Tables	vi
Acronyms	viii
1 Introduction	1
1.1 Theoretical Introduction	1
1.1.1 Characteristic x-rays	1
1.1.2 Transition Shape	3
1.2 Atomic Structure Calculations	4
1.2.1 The non-relativistic Hamiltonian	4
1.2.2 The Dirac Equation	5
1.2.3 The Dirac-Breit Equation	8
1.2.4 The <i>MCDFGME</i> Method	8
1.3 State of the Art	9
1.3.1 Copper's characteristic x-rays	9
1.3.2 <i>MCDFGME</i> capabilities	9
1.4 Objectives	9
1.5 Methodology	9
1.6 Work Plan	10
Bibliography	11
Appendices	
A The Breit Hamiltonian Equations	13
B Transition Diagram	14

List of Figures

1.1	Photoionization	2
1.3	Resonant Photoexcitation	4
1.4	Diagram	6
B.1	Transition notation scheme. Adapted from [1]	14

List of Tables

1.1 Siegbahn VS IUPAC notation. Adapted from [1]	3
--	---

Acronyms

MCDFGME Multiconfiguration Dirac-Fock General Matrix of Elements (*pp.* [ii](#), [iv](#), [8–10](#))

DCS Double Crystal Spectrometer (*p.* [ii](#))

FAC Flexible Atomic Code (*p.* [9](#))

Introduction

1.1 Theoretical Introduction

1.1.1 Characteristic x-rays

1.1.1.1 Ionization as a vacancy generator

When an atomic system is in a stable state, the electrons orbiting the nucleus will be occupying fixed quantum states, defined by their principal atomic number, n , angular momentum, l , and spin, s . Electrons are also fermions, they must respect Pauli's exclusion principle, each occupying a single state, only occupied by that single electron. These quantum numbers will provide information of their specific electron's wavefunction, which, when evaluated by operation of the Hamiltonian, will yield that state's energy.

Furthermore, beside the occupied states, more energetic unoccupied states will still be part of the systems eigenfunctions basis. The work performed in this thesis will explore what would happen should the system experience a perturbation that changes what the occupied and unoccupied states are, while still preserving the particles within it.

X-ray fluorescence spectroscopy has its many uses and applications in a wide range of scientific areas. In this form of spectroscopy, the element at study, composed of the nucleus and N orbiting electrons, are bombarded with x-rays, leading to the photoionization of inner-shell electrons, leaving a vacancy where the ejected electron used to be.

The atomic structure, now composed of $N - 1$ electrons will be left in an energetically unstable state, due to there being other possible less energetic configurations. This will lead to processes of atomic relaxation, where the system will be rearranged in order to find a more energetically favorable configuration.

The main processes for this rearrangement are two different competing processes, radiative relaxation, where an electron from a less bound orbital changes state in order to now occupy the one where the vacancy was, emitting an x-ray photon of characteristic energy, allowing for the easy identification of the element at study. The other competing process, the non-radiative relaxation, more commonly known as the Auger process, will still have the electron transit between states, but where before a photon was emitted, now

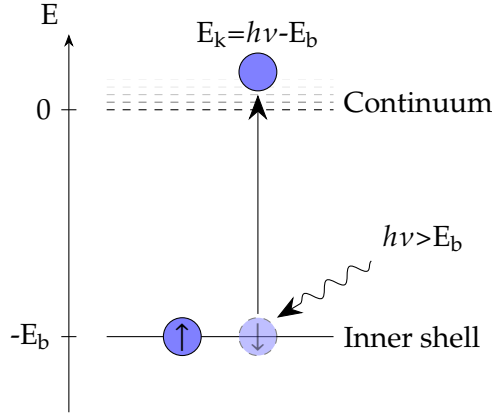
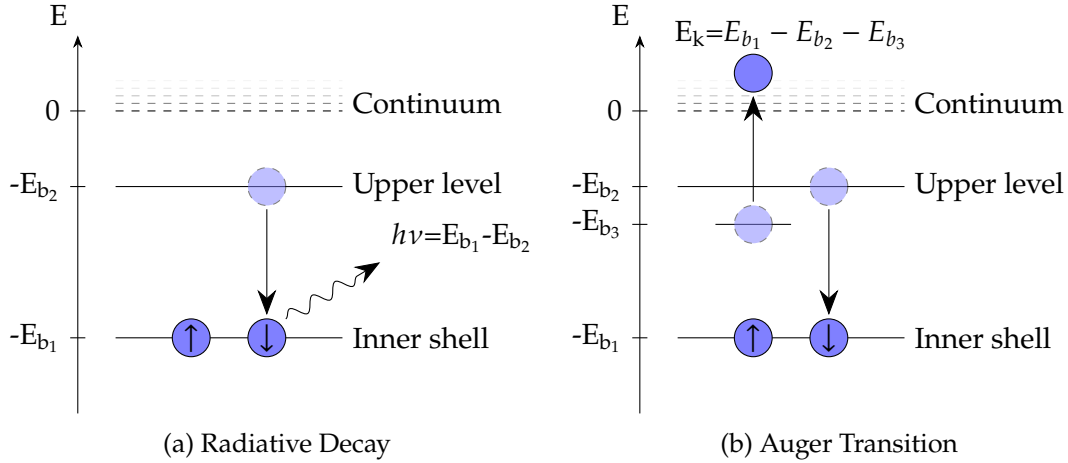


Figure 1.1: Photoionization

a new ionization will occur, where a weakly bound electron will leave to the continuum.



In reality, when the initial vacancy is generated due to an ionization, two more processes can occur: Shake-offs and shake-ups. When this processes occur, during the ionization, one other electron may become unbound, occurring a second ionization, in the shake-off process, or may be excited to an upper state, during shake-up. These processes occur due to the fact that the system, while it may have had a set of eigenstates before ionization, was changed when an electron was removed, leading to a change in the Hamiltonian, and the new system not being able to be accurately described by the previous system's states. These processes, however will not be studied through this thesis, due to the work in question not dealing with an initial ionization, but with an excitation, as it will be possible to understand in section 1.1.1.3.

1.1.1.2 Transition notation

The characteristic radiation obtained from the electronic structure relaxation of a post-ionization unstable atomic system is one of the main ways of identifying an atomic element, due to the photons emitted from different elements possessing some distinct values of

energy, forming well-defined energy lines when observed in a spectrometer. These lines have specific notations denoting them by vacancy/hole and the electron's orbital. A very illustrative diagram, exemplifying some transitions can be found in Appendix B.

Throughtout this thesis, mostly Siegbahn notation will be used, but should the reader prefer IUPAC's notation, one can convert one into the other using the following Table 1.1.

Table 1.1: Siegbahn VS IUPAC notation. Adapted from [1]

Siegbahn	IUPAC	Siegbahn	IUPAC	Siegbahn	IUPAC
K_{α_1}	$K - L_3$	L_{α_1}	$L_3 - M_5$	L_{γ_1}	$L_2 - N_4$
K_{α_2}	$K - L_2$	L_{α_2}	$L_3 - M_4$	L_{γ_2}	$L_1 - N_1$
K_{β_1}	$K - M_3$	L_{β_1}	$L_2 - M_4$	L_{γ_3}	$L_1 - N_2$
$K_{\beta_2}^I$	$K - N_3$	L_{β_2}	$L_3 - N_5$	L_{γ_4}	$L_1 - O_3$
$K_{\beta_2}^{II}$	$K - N_2$	L_{β_3}	$L_1 - M_3$	L_{γ_4}'	$L_1 - O_2$
K_{β_3}	$K - M_2$	L_{β_4}	$L_1 - M_2$	L_{γ_5}	$L_2 - N_1$
$K_{\beta_4}^I$	$K - N_5$	L_{β_5}	$L_3 - O_{4,5}$	L_{γ_5}	$L_2 - O_4$
$K_{\beta_4}^{II}$	$K - N_4$	L_{β_6}	$L_3 - N_1$	L_{γ_8}	$L_2 - O_1$
$K_{\beta_4}^x$	$K - N_4$	L_{β_7}	$L_3 - O_1$	L_{γ_8}'	$L_2 - N_{5,6}$
$K_{\beta_5}^I$	$K - M_5$	L_{β_8}	$L_3 - N_{6,7}$	L_{η}	$L_2 - M_1$
$K_{\beta_4}^{II}$	$K - M_4$	L_{β_9}	$L_1 - M_5$	L_l	$L_3 - M_1$
		L_{β_9}	$L_1 - M_4$	L_s	$L_3 - M_3$
		L_{β_9}	$L_3 - N_4$	L_t	$L_3 - M_2$
		L_{β_9}	$L_2 - M_3$	L_u	$L_3 - N_{6,7}$
				L_v	$L_2 - N_{6,7}$

1.1.1.3 Excitation as a vacancy generator

As previously mentioned, thought this thesis, while the study is focused on the characteristic radiation emitted during the atomic relaxation process, the vacancy generation method will be due to an excitation (Figure 1.3), instead of an ionization. This is one possibility of the many so-called satellite states, where the electronic configuration present during the relaxation process is not the commonly considered ground state ionization. The characteristic radiation from these states, may be one of the keys needed in order to fully comprehend and deconvolute an element's emission spectra.

1.1.2 Transition Shape

Falar de larguras, intensidades, raios de populaçao P1/2 P3/2, 2 photonblabla, monopolaes, quadrapolaes, etcect

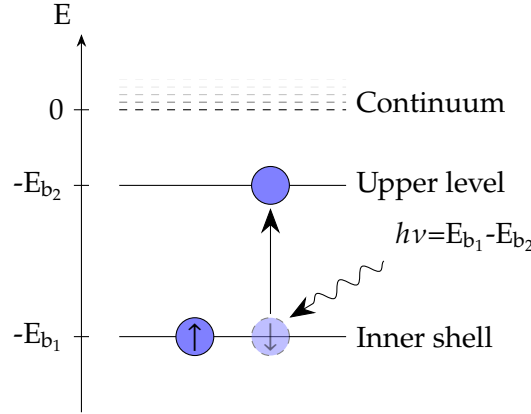


Figure 1.3: Resonant Photoexcitation

1.2 Atomic Structure Calculations

When studying a system composed of multiple charged bodies, one must consider all the existing interactions. Whilst there are known solutions for the 2-bodies Hydrogenoid systems, with the presence of more non spatially-bound particles (for example an electron, while using the Born-Oppenheimer approximation where the nuclei are considered at rest at a fixed position) there is just no analytic solution for the Schrödinger Equation. That way, there was a need for the development of numerical solutions able to solve this problem.

1.2.1 The non-relativistic Hamiltonian

The first approach used in order to solve the many-bodies problem used a non-relativistic consideration. This way, the used Hamiltonian consisted on simply the sum of the system's non-relativistic momentum-related energies and the Coulomb interactions between bodies, while still considering the Born-Oppenheimer approximation.

Essentially, and in atomic units:

$$H = \underbrace{\sum_i^N \frac{1}{2} \nabla_i^2 - \frac{Z}{r_i}}_{\text{Individual Hamiltonian}} + \underbrace{\sum_{i < j}^j \frac{1}{r_{ij}}}_{\text{Pair repulsion}} \quad (1.1)$$

1.2.1.1 The Hartree-Fock Method

Hartree developed an iterative method, further enhanced by Fock and Slater, based on the field self-consistency method.

In this method, while studying a multi-electronic system, such as an atom, each electron's wavefunction is composed as a product of a spacial part, ψ , and one indicating the electron's spin, χ , as to account for Pauli's exclusion principle.

$$u = \psi\chi \quad (1.2)$$

The wavefunction capable of describing the whole system, Ψ , should be somewhat of a product of all the wavefunctions describing each individual electron. However, one must not forget the need for this wavefunction respect the antisymmetry principle, due to the electron's fermionic nature. In order to respect this, Ψ is to be composed of a Slater determinant:

$$\Psi = \frac{1}{\sqrt{N!}} \begin{vmatrix} u_1(x_1) & u_2(x_1) & \cdots & u_N(x_1) \\ u_1(x_2) & u_2(x_2) & \cdots & u_N(x_2) \\ \vdots & \vdots & \ddots & \vdots \\ u_1(x_N) & u_2(x_N) & \cdots & u_N(x_N) \end{vmatrix} \quad (1.3)$$

It is of high importance that the wavefunctions must form an orthonormal basis. These are to be initialized as trial wavefunctions.

The main goal of this method is to follow the variational principle and to minimize a functional, with the purpose of minimizing the system's energy. Assuming the optimal, yet unknown energy, E_0 (calculated by Operating the Hamiltonian on the optimal wavefunctions), it is natural to assume the used test functions provide a non-minimized solution, with $\langle \Psi | H | \Psi \rangle \geq E_0$.

The computational method consists on starting with the previously mentioned test wavefunctions, using them to calculate Hartree-Fock's potential through the HF equations,

In a very simplified way, the self-consistent Hartree-Fock computational method can be represented by the following block diagram:

1.2.2 The Dirac Equation

It is no secret that the Schrödinger equation has some very considerable limitations. The fact that it does not account for the existence of the electron's spin and the lack of consideration of relativistic effects are some of the most impactful setbacks.

That way, a new equation was developed by Paul Dirac, in 1928[2], one taking into account now not the classical 3 dimensional space components, but the relativistic four components (1 time-like and 3 space-like).

Many scientists, such as Klein, Gordon and later Fock, had already conceived a relativistic correction to Schrödinger's equation, more commonly known as the Klein-Gordon equation(1.6), where the free-particle energy makes use of the relativistic momentum-energy relation (1.4), making Schrödinger's equation now also Lorentz-invariant. This new approach was, however, still faulty, due to only describing spin 0 particles (e.g., some mesons), and making use of a second order derivative in the time-like component.

$$E = \sqrt{c^2 p^2 + m^2 c^4} \quad (1.4)$$

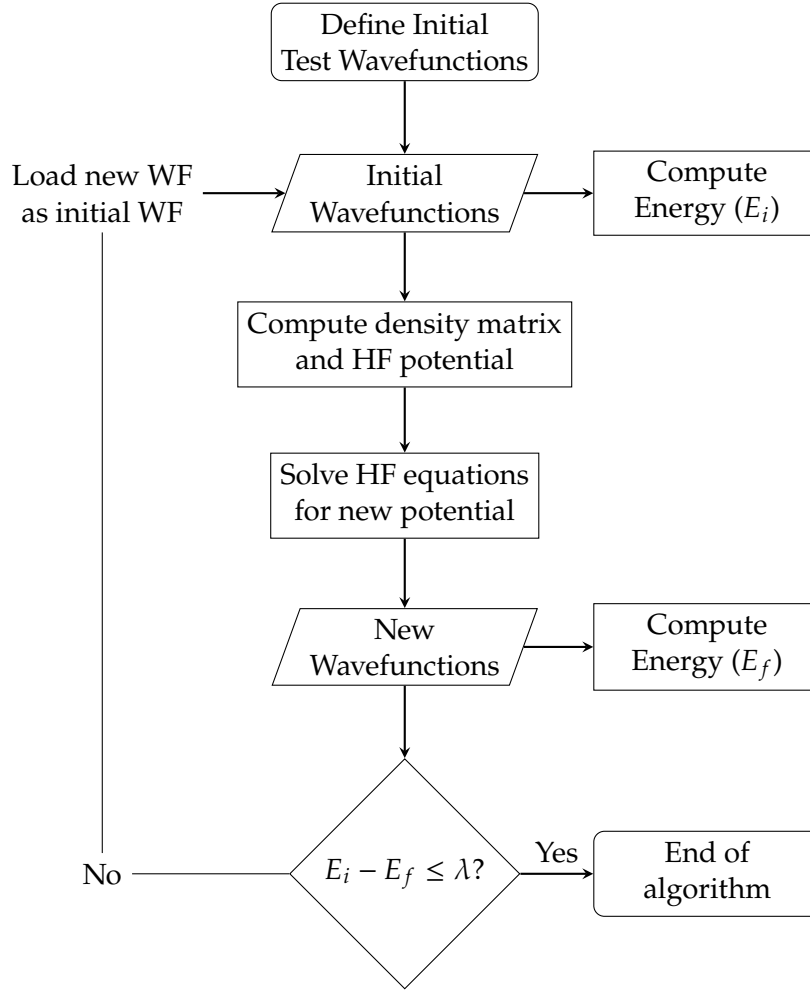


Figure 1.4: Diagram

Which can be derived from:

$$\frac{E^2}{c^2} = \mathbf{p}^2 + m^2 c^2 \Leftrightarrow \frac{E^2}{c^2} - \mathbf{p}^2 = m^2 c^2 \Leftrightarrow p^\mu p_\mu = m^2 c^2 \quad (1.5)$$

Just as a reminder, since now relativistic effects are being taken into account, the momentum vector is now a 4-vector, composed of one time-like and 3 space-like components: $p^\mu = (p^0, p^1, p^2, p^3) = (p^0, \mathbf{p}) = \left(\frac{E}{c}, \mathbf{p}\right)$

$$-\hbar^2 \frac{\partial^2}{\partial t^2} \psi = -c^2 \hbar^2 \nabla^2 + m^2 c^4 \psi \quad (1.6)$$

Dirac took a spin at rewriting the energy-momentum relation, ending up with an equivalent equation(1.7), involving 4×4 matrices, due to the 4 relativistic dimensions at play, and incorporating spins into the equation by making use of the now famous Pauli matrices, σ :

$$E = c \boldsymbol{\alpha} \cdot \mathbf{p} + \beta m c^2, \quad \boldsymbol{\alpha} = (\alpha_1, \alpha_2, \alpha_3) \quad (1.7)$$

$$\alpha_i = \begin{pmatrix} 0 & \sigma_i \\ \sigma_i & 0 \end{pmatrix} \quad \beta = \begin{pmatrix} I_2 & 0 \\ 0 & -I_2 \end{pmatrix} \quad I_2 = \begin{pmatrix} 1 & 0 \\ 0 & 1 \end{pmatrix} \quad (1.8)$$

$$\sigma_1 = \begin{pmatrix} 0 & 1 \\ 1 & 0 \end{pmatrix} \quad \sigma_2 = \begin{pmatrix} 0 & -i \\ i & 0 \end{pmatrix} \quad \sigma_3 = \begin{pmatrix} 1 & 0 \\ 0 & -1 \end{pmatrix} \quad (1.9)$$

In order to fully comprehend this shift of notation, one should equate the square of the two equations, (1.4) and (1.7), and confirm if logic still stands.

$$c^2 \mathbf{p}^2 + m^2 c^4 = c^2 \boldsymbol{\alpha}^2 \mathbf{p}^2 + 2mc^3 \boldsymbol{\alpha} \cdot \mathbf{p} \cdot \beta + \beta^2 m^2 c^4 \quad (1.10)$$

In order for this equation to make sense, the following conditions must be true (which in fact, they are):

$$\begin{cases} c^2 \mathbf{p}^2 = c^2 \boldsymbol{\alpha}^2 \mathbf{p}^2 & \Leftrightarrow \boldsymbol{\alpha}^2 = 1 \\ 0 = 2mc^3 \boldsymbol{\alpha} \cdot \mathbf{p} & \Leftrightarrow \boldsymbol{\alpha} \cdot \mathbf{p} = 0 \\ m^2 c^4 = \beta^2 m^2 c^4 & \Leftrightarrow \beta^2 = 1 \end{cases} \quad (1.11)$$

As expected, the eigenfunctions obtained from solving this equation, will now have a 4th time-like component, in addition to the already expected 3 space-like components.

With all the previous considerations taken into account, one can now construct Dirac's free-particle equation(1.12):

$$i\hbar \frac{\partial}{\partial t} \psi = (c \boldsymbol{\alpha} \cdot \mathbf{p} + \beta mc^2) \psi = \begin{pmatrix} mc^2 I_2 & -i\hbar c \boldsymbol{\sigma} \cdot \nabla \\ -i\hbar c \boldsymbol{\sigma} \cdot \nabla & -mc^2 I_2 \end{pmatrix} \cdot \begin{pmatrix} \psi_1 \\ \vdots \\ \psi_4 \end{pmatrix} \quad (1.12)$$

This equation, however, as previously mentioned above, can only describe a single particle present in a field-free region. In order to account for the existence of a field, such as the electromagnetic field, derived from the four-potential A^μ , composed by the electric scalar potential, $A^0 = \phi$, and the vector potential, $(A^1, A^2, A^3) = \mathbf{A}$:

$$p^\mu \rightarrow p^\mu - eA^\mu, \quad A^\mu = (\phi, \mathbf{A}) \quad (1.13)$$

The Hamiltonian can now be rewritten as to account for the presence of the electromagnetic field (1.14). This way it is possible to include, for example, the electron-nucleus Coulomb attraction.

$$H_D = -e\phi + \beta mc^2 + \boldsymbol{\alpha}(c\mathbf{p} + e\mathbf{A}) \quad (1.14)$$

For a central potential, as is the one generated by the nuclear charge, the 3 space-like components from the four-potential are null, and the time-like component, $\phi = \frac{Ze}{r}$. The equation gains now a more recognizable term:

$$H_D = -\frac{e^2 Z}{r} + \beta mc^2 + \boldsymbol{\alpha} \cdot \mathbf{p} c \quad (1.15)$$

A very interesting fact about this equation is that one does not obtain a simple solution. In fact solving this equation yields two different solutions, one for particles, and another one for antiparticles, commonly named large and small components.

1.2.3 The Dirac-Breit Equation

Once again, when considering a system composed of many bodies, one must consider all the present interactions, namely, the electron-electron repulsion in an atom. Breit, in 1929, had already created a relativistic approach to treat the electron-electron interactions, consisting on a set of equations building upon the classical non-relativistic Hamiltonian from equation (1.1), which can be consulted in Appendix A. Breit's equations are able to account for angular momenta couplings and estimate level energy splittings, the change of a particle's apparent mass as a function of velocity, and even include the interaction of an applied external magnetic field.[3]

It is quite obvious Breit's equations introduce a great complexity in the search of the new Hamiltonian's eigenfunctions. However, when trying to include an approximation of Breit's considerations into Dirac's equation, one must add the following operator to the one present in equation (1.15):

$$H_B = \sum_{i>j} \frac{e^2}{r_{ij}} - e^2 \left(\frac{\boldsymbol{\alpha}_i \boldsymbol{\alpha}_j}{r_{ij}} + \frac{(\boldsymbol{\alpha}_i \nabla_i)(\boldsymbol{\alpha}_j \nabla_j) r_{ij}}{2} \right) \quad (1.16)$$

This set of terms will account for the fact that Coulomb interactions, mediated by the electric field, and therefore, virtual photons, can not occur at instantaneous velocities, but at the speed of light.

1.2.4 The *MCDFGME* Method

As previously mentioned in section 1.2.1.1, there is a need for a numerical method in order to compute and find the eigenfunctions for a many-body Hamiltonian. While the Hartree-Fock method was able to reasonably solve the non-relativistic problem, now, while considering the Dirac-Breit Hamiltonian from equations (1.15) and (1.16), there is a need for a new method.

Hence, the state of the art *MCDFGME* arises. This self-consistent iterative method, based on the same method present in section 1.2.1.1, is able to solve and find eigenfunctions for a multielectronic system, now taking into account the Dirac-Breit Hamiltonian. Moreover, it is also capable of incorporating electron correlation and many QED effects not yet considered in the relativistic equation, such as the Lamb-shift, vacuum polarization, and the electron's self energy. A brief description of these contributions can be found in appendix ???

EXPLICAR A GENERAL MATRIX OF ELEMENTS.

1.3 State of the Art

1.3.1 Copper's characteristic x-rays

1.3.2 MCDFGME capabilities

It has been noted multiple times that *MCDFGME* code thrives in atomic structure calculations of super-heavy elements and highly-charged ions, where relativistic and QED effects are in prevalence [4–6]. However, it has also been proven to be an excellent tool for the calculation of less ionized systems [7].

In addition, the *MCDFGME* is able to calculate radiative and auger transition rates for the calculated configurations, leading to the possibility to yield results that can be used in the simulation of Theoretical spectra, due to being able to provide the transition's intensity and natural width. Since it is able to perform calculations even for exotic atoms, it can be used to further understand many QED phenomena, aiding in the theoretical calculations supporting experimental data [8].

It should also be of note that there are many other code alternatives. While *MCDFGME*, which is a close-source project, provides a very high precision in the performed calculations at a high computational cost, *Flexible Atomic Code (FAC)*, is an open source code which requires less computational time for the calculations, however, it lacks *MCDFGME*'s precision, since it only is able to consider all the spin-orb couplings, but not the possible configurations originating them. It can, however, calculate other collisional processes, such as electronic impact excitation cross-sections [9]

1.4 Objectives

1.5 Methodology

As previously mentioned before, in this thesis, atomic relaxation transitions where the ejected inner shell electron, responsible for the generated hole, was, not sent to the continuum, but excited to an upper state.

In order to use *MCDFGME*, since it is written in FORTRAN, there will be a multitude of I/O files, with the extension .f0X. The most important file extensions are .f05, the input file, where the calculation settings are indicated; .f06, where the cyclical energy results will be displayed, among others, such as the non-diagonal matrix element overlaps, both important to evaluate the convergence. Other file extensions, such as .f09 can be quite useful for debugging processes, and for calculating other atomic parameters, such as shake probabilities, which will not be of relevance as of this thesis.

An example of a normal atomic structure calculation for an excited Copper atom (which has a ground state configuration of $1s^2 2s^2 2p^6 3s^2 3p^6 3d^{10} 4s^1$) is as follows:

One starts by choosing the excitation upper orbital, and by writing, in a text file all the possible 1 hole configurations from where the electron may have originated from. An

example can be found in Annex ????. This represents all the possible excited states where the electron is in the chose orbital.

The same process is now performed for a 2 hole configuration, where an additional ionization occurred. This represents the possible states after the occurrence of the Auger process, which is in competition with the radiative decay.

Now, a *bash* script, *runMCDFEC.sh* is to be executed. Now, it will be possible to choose the atomic number of the element in study, the isotope mass, and, if one wishes so, to perform the calculations for an exotic atom, where, instead of electrons, other particles such as muons, negative hadrons and antiparticles can orbit the nucleus. The script will, for all given configurations, calculate all the possible spin-orbit couplings and eigenvalues, and then finally apply the *MCDFGME* method.

Depending on the excitation orbital, there will be thousands to tens of thousands of possibilities for the final configuration, with this number increasing with the quantum number of angular momentum, l , of the orbital.

However, not all the calculations automatically performed will converge. Each time, a couple of hundreds of computed orbitals will fail convergence. In a file, generated for the compilation of the calculation results, these orbitals will be missing the total system's energy, or will display a significant energy difference for the results of using two different methods, **breaking the method's self-consistency???**.

The configurations that were not able to converge will now have to be converged by hand. In order to do this, their *f05* will have to be edited, where different methods will be chosen for the calculation for each specific orbital. This can be quite time-consuming, as there are multiple possible methods and possible combinations, and there is just no right way to converge an orbital, hence why this step can even take a couple of weeks to finish.

After eliminating all the convergence problems, the radiative transition rates will be calculated, by operating the transition operator on all the possible 1 hole - 1 hole configuration pair combinations. The same will follow for all the pairs of 1hole - 2 holes configurations, in order to compute the auger transition rates. Finally, the process is repeated for the 2 holes - 2 holes configurations, for the radiative transitions of the auger-generated satellite states.

The energy of the transition is calculated through the configuration pair's energetic difference, and the transition's natural broadening by:

1.6 Work Plan

The work performed in this thesis will

Bibliography

- [1] M. F. Vitha, R. Klockenkämper, and A. V. Bohlen. *Chemical Analysis: A Series of Monographs on Analytical Chemistry and Its Applications Total-Reflection X-ray Fluorescence Analysis and Related Methods SECOND EDITION*. Ed. by M. Vitha. 2nd. Vol. 181. 2015, pp. 20–21 (cit. on pp. 3, 14).
- [2] P. A. M. Dirac. “The quantum theory of the electron”. In: *Proceedings of the Royal Society of London. Series A, Containing Papers of a Mathematical and Physical Character* 117 (778 1928-02), pp. 610–624. ISSN: 0950-1207. DOI: [10.1098/rspa.1928.0023](https://doi.org/10.1098/rspa.1928.0023) (cit. on p. 5).
- [3] H. A. Bethe and E. E. Salpeter. *Quantum Mechanics of One- and Two-Electron Atoms*. Springer US, 1977. DOI: [10.1007/978-1-4613-4104-8](https://doi.org/10.1007/978-1-4613-4104-8) (cit. on p. 8).
- [4] P. Indelicato, J. Bieroń, and P. Jönsson. “Are MCDF calculations 101% correct in the super-heavy elements range?” In: *Theoretical Chemistry Accounts* 129 (3-5 2011-06), pp. 495–505. ISSN: 1432881X. DOI: [10.1007/s00214-010-0887-3](https://doi.org/10.1007/s00214-010-0887-3) (cit. on p. 9).
- [5] P. Indelicato, O. Gorceix, and J. P. Desclaux. “Multiconfigurational Dirac-Fock studies of two-electron ions. II. Radiative corrections and comparison with experiment”. In: *Journal of Physics B: Atomic and Molecular Physics* 20 (4 1987-02), p. 651. ISSN: 0022-3700. DOI: [10.1088/0022-3700/20/4/007](https://doi.org/10.1088/0022-3700/20/4/007) (cit. on p. 9).
- [6] O. Gorceix, P. Indelicato, and J. P. Desclaux. “Multiconfiguration Dirac-Fock studies of two-electron ions. I. Electron-electron interaction”. In: *Journal of Physics B: Atomic and Molecular Physics* 20 (4 1987-02), pp. 639–649. ISSN: 00223700. DOI: [10.1088/0022-3700/20/4/006](https://doi.org/10.1088/0022-3700/20/4/006) (cit. on p. 9).
- [7] M. Guerra et al. “Fundamental Parameters Related to Selenium K α and K β Emission X-ray Spectra”. In: *Atoms* 9 (1 2021-01), p. 8. ISSN: 2218-2004. DOI: [10.3390/atoms9010008](https://doi.org/10.3390/atoms9010008). URL: <https://www.mdpi.com/2218-2004/9/1/8> (cit. on p. 9).
- [8] N. Paul et al. “Testing Quantum Electrodynamics with Exotic Atoms”. In: *Physical Review Letters* 126 (17 2021-04), p. 173001. ISSN: 10797114. DOI: [10.1103/PhysRevLett.126.173001](https://doi.org/10.1103/PhysRevLett.126.173001) (cit. on p. 9).

BIBLIOGRAPHY

- [9] M. F. Gu. *The flexible atomic code*. 2008-05. DOI: [10.1139/P07-197](https://doi.org/10.1139/P07-197) (cit. on p. 9).

The Breit Hamiltonian Equations

Note: This equations are valid for the electrons in an atom.

The free particle energy:

$$H_0 = \sum_i^N \frac{p_i^2}{2m_e} \quad (\text{A.1})$$

The electron-nucleus Coulomb attraction:

$$H_1 = \sum_i^N -\frac{e^2 Z}{r_i} \quad (\text{A.2})$$

The electron-electron Coulomb repulsion:

$$H_2 = \sum_{i>j} \frac{e^2}{r_{ij}} \quad (\text{A.3})$$

asdkjhdaikhdsajdhjska:

$$H_3 = -\frac{1}{8m_e^3 c^2} \sum_i^N p_i^4 \quad (\text{A.4})$$

ACABAR O RESTO

Transition Diagram

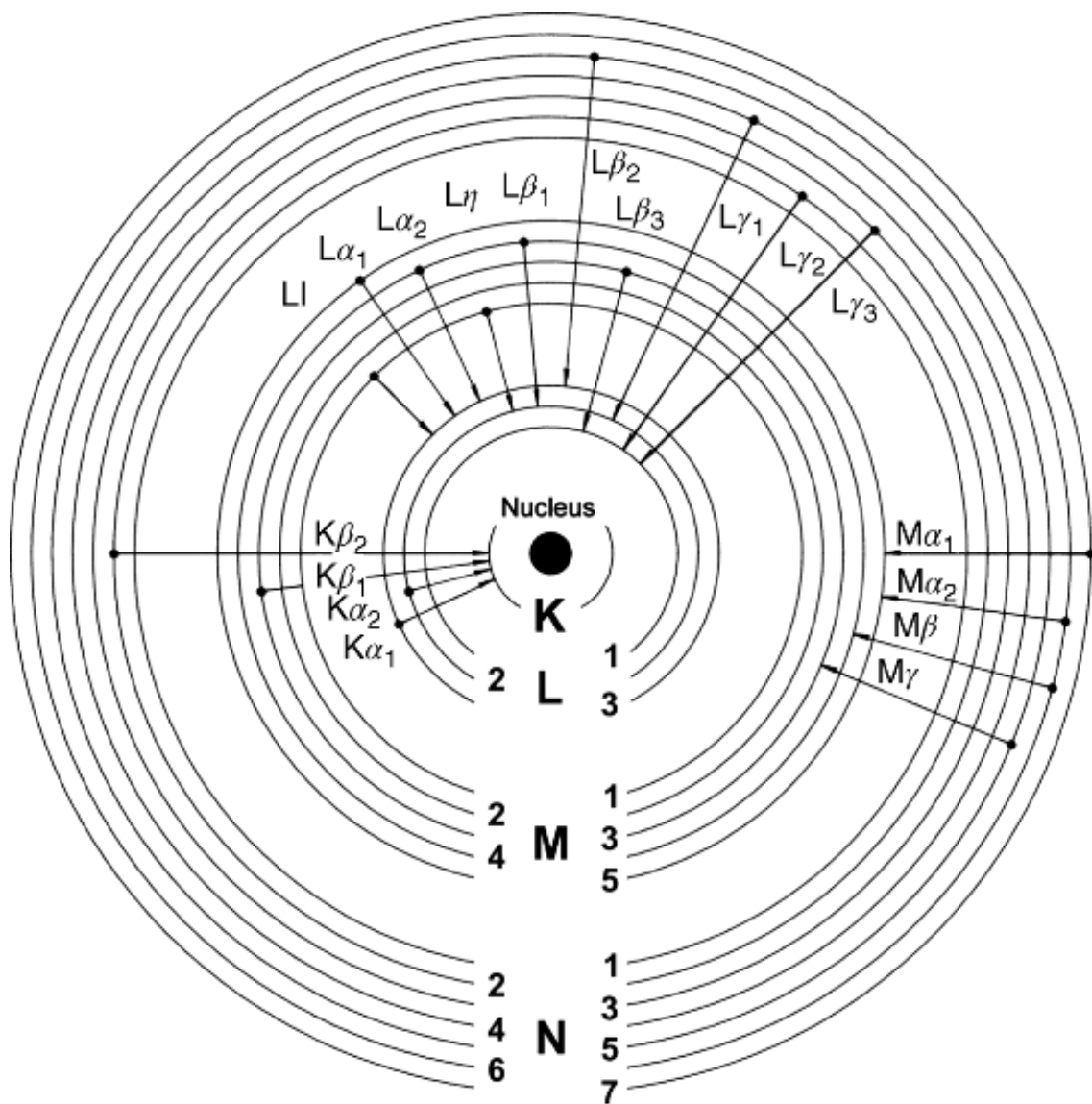


Figure B.1: Transition notation scheme. Adapted from [1]





Quantifying Raman Scattering Gonçalo Baptista

Quantifying Raman Scattering Gonçalo Baptista